

Electrochemical Synthesis of Polyaniline on Onion-like Carbon Nanoparticles using the Rotating Disk Slurry Electrode Technique

B. L. Vargas-Pérez^a, F. N. Sánchez-Fonseca^a, K. M. Gonzalez-Aponte^a, and L. Cunci^a

^a School of Natural Sciences and Technology, Universidad Ana G. Méndez-Gurabo Campus, Gurabo, Puerto Rico 00778

The main source of energy in the world is fossil fuels, but these can irreparably harm the environment. My research focuses on making a catalyst that is economical, efficient, and environmentally friendly. The oxygen reduction reaction is an important reaction for energy conversion systems, such as fuel cells. Onion-like carbon nanoparticles are used as a catalytic support for fuel cell applications due to its high conductivity and surface-to-volume ratio. The combination of carbon compounds with conductive polymers results in new materials and devices with possible practical applications. In my research we obtain onion-like carbon from nanodiamonds through a pyrolysis process. These particles are then polymerized using the aniline monomer to dope the OLCs with nitrogen. These particles are characterized by different characterization techniques such as Raman and Fourier transform infrared spectroscopy and scanning electron microscopy. After characterizing them, electrochemical experiments were carried out.

Introduction

In 1992, onion-like carbon (OLC) nanoparticles, which are also known as carbon nano-onions, were discovered by Ugarte (1-3). This carbon allotrope consists of an inner layer of 60 carbon atoms and several other carbon layers increasing by $60n^2$ the number of carbons with n being the number of layers (2). OLC are synthesized starting from nanodiamonds in a high temperature oven (1). OLC have several applications including their use as catalytic support for fuel cells given that they have higher specific surface area than single-walled carbon nanotubes. In this work, OLC will be used as a support together with conductive polymers for the synthesis of a composite. The fabrication of composites using carbon materials as a support increases the effective utilization of the active materials and improve the electrical conductivity of the catalytic layer in the electrodes. Moreover, the combination the conductive polymers with OLC is also more attractive to reinforce their mechanical properties (3,4). In this work, given that we aimed to dope OLC with nitrogen, the conductive polymer that was used was polyaniline (PANI) synthesized from aniline as the monomer since it contains a nitrogen atom in the molecule and can be

polymerized electrochemically. PANI exhibits relatively high conductivity, good stability in water and air, and relatively low cost (3, 5-7). Therefore, PANI was selected to be used for the nitrogen doping. Nitrogen-doped carbon nanoparticles can be used as a catalytic support or by itself as a low-cost catalyst for the oxygen reduction reaction (ORR), which represents a key, although sluggish, reaction at the cathode of some proton exchange membrane fuel cells, microbial fuel cells, and metal air batteries (8-14).

The rotating disk slurry electrode (RoDSE) technique has been used to deposit isolated atoms and metallic particles on unsupported nanocarbon materials (15, 16). Furthermore, this technique is used to prepare carbon-supported catalysts such as Vulcan XC-72, nanotube, nano-onions, and graphene oxide (16). In our work, this technique was used to dope OLC particles with nitrogen in order to create more economical and environmentally friendly catalysts for the ORR. Through this technique, a potential range was applied where the oxidation and reduction of the aniline monomer occurred. In this way, the use of oxidizing agents is avoided, making it a more environmentally friendly process. One of the advantages of carrying out the aniline polymerization with this technique is that it improves the mechanical properties of the polymer, having a higher conductivity (3, 17). With this technique, OLC are deposited with PANI in order to increase their surface area by covering the pores that obstruct the metallic particles. This improves the properties of the catalyst.

Experimental Section

Preparation of Onion-like Carbon Nanoparticles

Raw OLC were obtained by annealing nanodiamond (ND) powder under a positive pressure of helium at 1,650 °C (18). Oxidized OLC were prepared by treating raw OLC with concentrate sulfuric acid and six times potassium permanganate of the amount needed to oxidize OLC. The temperature was set to 50 °C, and the mixture was left stirring for 4 days. Then, the solution was poured slowly into cold deionized water. In addition, 10 mL of 35% H₂O₂ was added dropwise.

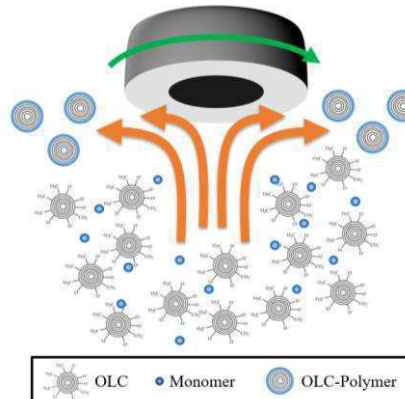


Figure 1 – Schematic of the RoDSE technique process.

Electrochemical Synthesis of OLC/PANI

Oxidized OLC were doped with PANI electrochemically. A solution of 50 mg OLC, 0.17 M aniline, and 0.1 M H₂SO₄ was prepared. The synthesis done was using the RoDSE technique. The potential range used was between -0.2 V and 0.8 V vs Ag|AgCl. The conditions for the cyclic voltammetry were 100 mV/s, 300 cycles, 900 rpm, after a pre-treatment bubbling the solution using dry N₂. The working electrode is glassy carbon electrode. The potentiostat used was a GAMRY Instruments Reference 600+ and WaveVortex 10 Electrode Rotator of PINE Research, was a rotating glassy carbon disk electrode from PINE Research.

Characterization Techniques

Raman spectroscopy was performed using a DXR 3 Raman imaging microscope from ThermoFisher Scientific. This was used to observe changes in the structure of the OLCs. Fourier-transform infrared spectroscopy (FTIR) was performed to identify the different functionalities. JEOL JSM-6010LA scanning electron microscopy (SEM) was used to determine the changes in the morphology of the electrochemical synthesis with energy-dispersive X-ray spectroscopy (EDS). A FEI F20 TEM STEM transmission electron microscope (TEM) was used to study the structure of the samples.

Results

Figure 2 shows the electrochemical synthesis of OLC/PANI composites. Figure 2 shows the electrodeposition using cyclic voltammetry with a potential range from (A) -0.2 V to 0.6 V, from (B) -0.2 V to 0.7 V, and from (C) -0.2 V to 0.8 V. It was expected that the polymerization of aniline was only going to proceed when a potential higher than 0.6 V was reached (19). The redox peaks of PANI are expected to be observed in the cyclic voltammetry of the rotating electrode only when the polymerization was successful, therefore, showing the possibility of the polymerization also on the surface of the OLC. Figure 2A shows the reduction and oxidation peaks at 0.01 V and 0.48 V for the initial cyclic voltammetry (CV) and the same peaks moved together in the final CV. The similarity of both results implies the lack of the polymerization of the aniline, given that these peaks only correspond to the redox reaction of quinone to o-quinone on the surface of the glassy carbon (3). Figure 2B, on the other hand, shows three reduction peaks at 0.05 V, 0.42 V and 0.58 V as well as three oxidation peaks at 0.20 V, 0.47 V, and 0.66 V which are related to the redox reaction of the PANI(3). Figure 2C shows a cyclic voltammetry where only two reduction peaks are clearly seen at 0.00 V and 0.47 V as well as two oxidation peaks at 0.33 V and 0.62 V. The electrical current measured was much higher compared to the cyclic voltammetry seen in Figure 2B due to the increased amount of polymerization that occurred when using a potential range up to 0.8 V. Moreover, each pair

of redox peaks separated due to the thicker polymer layer formed that increased the resistance while decreasing the reversibility of the reaction. The same three peaks as seen in Figure 2B should appear; however, they are overlapped and indistinguishable of each other as is shown by the widening and movement of the peaks. Figure 2B and Figure 2C showed a clear change in the electrode surface indicating that polymerization occurred in the electrode surface.

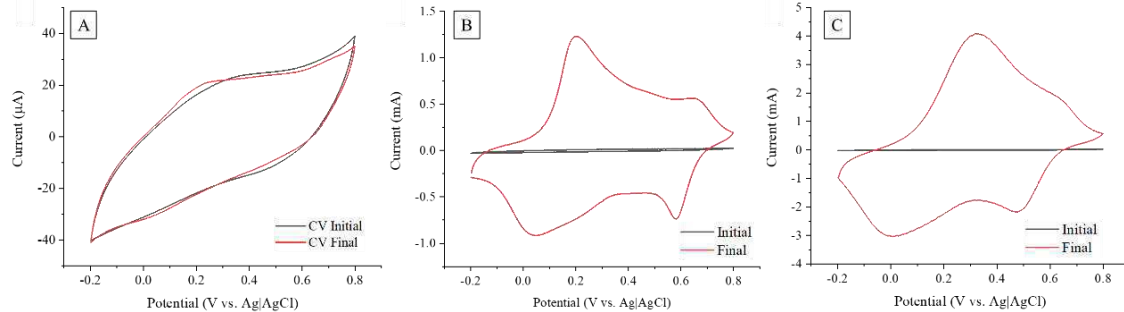


Figure 2 – Cyclic voltammetry of the polymerization of aniline using the RoDSE technique. (A) Potential ranges from -0.2 V to 0.6 V, (B) from -0.2 V to 0.7 V, and (C) from -0.2 V to 0.8 V.

EDS spectra of the polymerization of aniline on the OLC using the potential range from -0.2 V to 0.6 V is shown in Figure 3A. Figure 3B is the spectrum of the sample of OLC/PANI at -0.2 V to 0.7 V and Figure 3C corresponds to the polymerization made at -0.2 V to 0.8 V. We can observe the carbon peaks and oxygen peaks in each sample. The carbon peaks are at 0.28 keV and the oxygen peaks are at 0.53 keV. In the EDS spectrum we cannot observe the nitrogen peaks, which may be due to the amount of nitrogen that was deposited that is not enough to be detected by EDS. Therefore, we used additional characterization techniques to study this material.

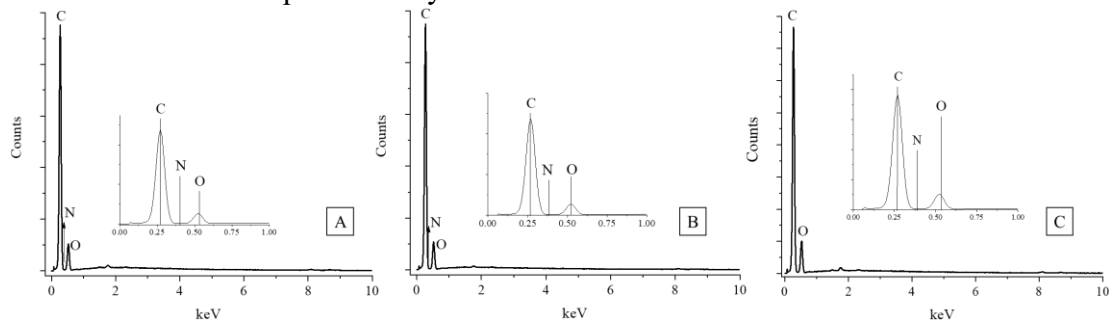


Figure 3 – EDS spectra of the polymerization of aniline in the OLC. (A) Potential range -0.2 V to 0.6 V, (B) potential range -0.2 V to 0.7 V and (C) potential range -0.2 V to 0.8 V.

Raman spectrum (Figure 4A) is very useful in confirming the presence of synthesized carbon nanomaterials of different structures. Figure 4A shows OLC raw, synthesized OLC, and the different potential ranges of OLC/PANI. The D and G bands are characteristic peaks of carbon nanomaterials. The D band is associated with the A_{1g} vibrational mode and has been attributed to the disorder induced in the structure due to presence of sp^3 carbons

(20). G band corresponds to the E_{2g} vibrational mode of the sp^2 carbon (1). The width of the G band is related to the disorder between the sheets of sp^2 hybridized carbon. The 2D band corresponds to different amounts of layers (18). The FTIR spectra seen in Figure 4B show the OLC raw, synthesized OLC and the different potential ranges of OLC/PANI. The peaks seen at 1580 cm^{-1} and 1490 cm^{-1} can be attributed to the stretching deformation of the benzenoid ring. The signal 1290 cm^{-1} and 1240 cm^{-1} correspond to C-N of the stretching of secondary aromatic amine and C-N⁺ of the stretching and vibration in the polaron structure of PANI, respectively. The last signal, 1150 cm^{-1} , correspond to the aromatic C-H in-plane bending.

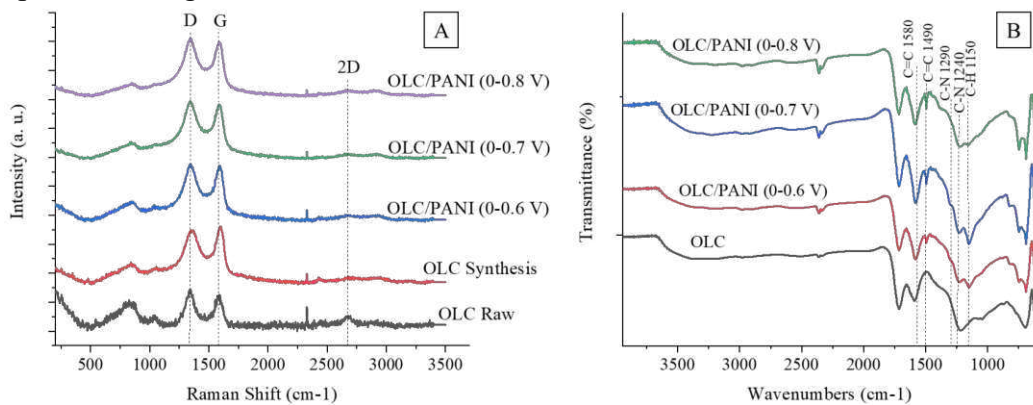


Figure 4 – (A) Raman spectroscopy and (B) FT-IR characterization of OLC/PANI.

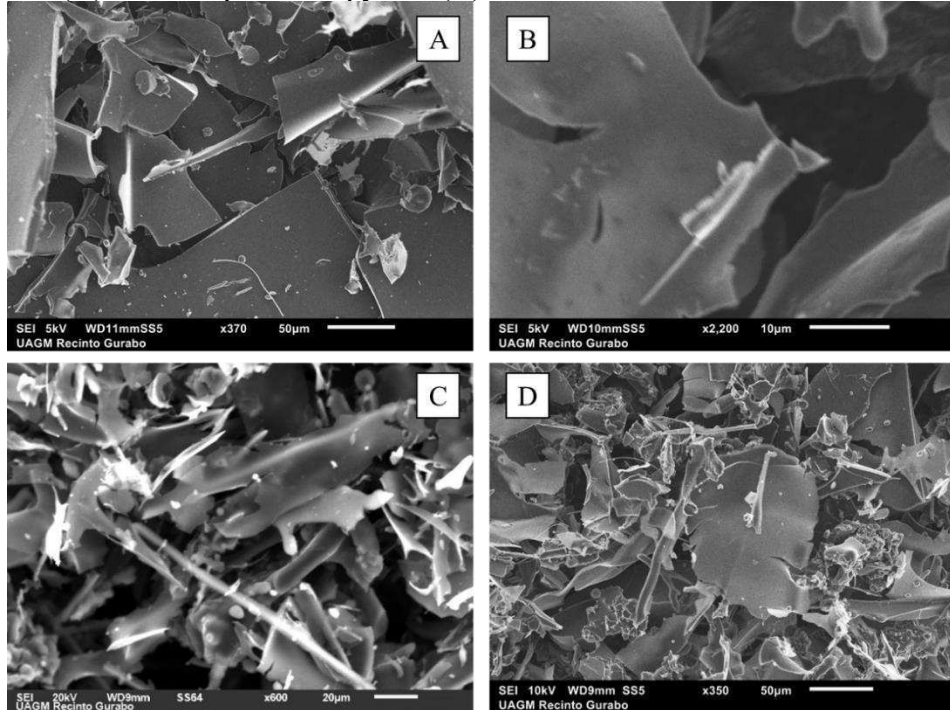


Figure 5 – SEM images for of (A) OLC Raw and OLC/PANI synthesized at potentials from (B) -0.2 V to 0.6 V, (C) from -0.2 to 0.7 V, and (D) from -0.2 V to 0.8 V.

Figure 5 shows the SEM images of the different samples. The Figure 5A is a SEM image of OLC synthesis before the polymerization process of aniline. Figure 5B-D present the samples of OLC/PANI synthesis at different potential ranges from -0.2 V to 0.6 V (Figure 5B), from -0.2 V to 0.7 V (Figure 5C), and from -0.2 V to 0.8 V (Figure 5D). As shown by the SEM images, the morphology of these samples is very similar to each other. In Figure 5A, Figure 5B, and Figure 5D we observe the layers of the very similar OLCs, but Figure 5C shows a sphere with a cover.

TEM images of different samples can be seen in Figure 6. Given that the samples synthesized up to 0.8 V was supposed to obtain the higher amount of PANI according to the CV shown in Figure 2C, we continued the characterization of the samples focusing on the polymerization made at higher potentials. Figure 6A is the sample of the OLC synthesis before of the polymerization process with the polymer. In this image, OLC can be seen with onion-shaped layers of carbon for which these carbon particles are known. On the other hand, Figure 6B corresponds to the sample of the synthesis of OLC/PANI from the potential range of -0.2V to 0.8 V. In this image, a material that covers the OLC is observed. This coverage corresponds to the organic compound of the polymer. The structure of the OLC underwent a change after going through the polymerization process using the RoDSE technique as seen in the TEM images.

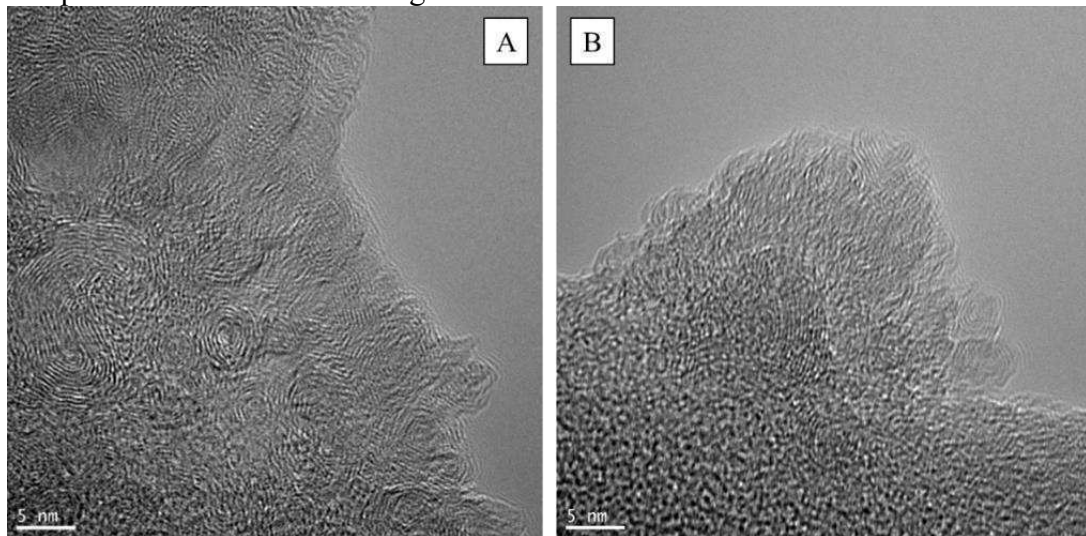


Figure 6 – TEM images of (A) OLC as synthesized and (B) OLC/PANI synthesis at -0.2 V to 0.8 V.

In the voltammogram, the cyclic voltammetry of glassy carbon electrode (GCE), OLC, and the sample of OLC/PANI that was synthesized up to 0.8 V. The potential limits of these experiments range from -0.2 V to 0.8 V vs Ag|AgCl, scan speed 100 mV/s, in a solution of 0.1 M H₂SO₄ after dry N₂ purging. The voltammogram of GCE and OLC are very similar showing just small variations between them given that both carbon materials are similar electrochemically. However, the cyclic voltammetry of

OLC/PAN synthesized using a potential range up to 0.8 V vs Ag|AgCl shows a clear change. Even though some techniques were not able to show a clear deposition of nitrogen containing molecules on the surface of the OLC, this cyclic voltammetry clearly showed the change on the surface of OLC. The voltammogram shows a small slope between 0.01 V and 0.37 V, which may be due to an increased resistance between those values due to the polymer coating. Moreover, the capacitance of the surface increased as seen by the separation of the anodic and cathodic currents. The measured electric current was much higher compared to the cyclic voltammetry of the OLCs due to the polymerization in these particles.

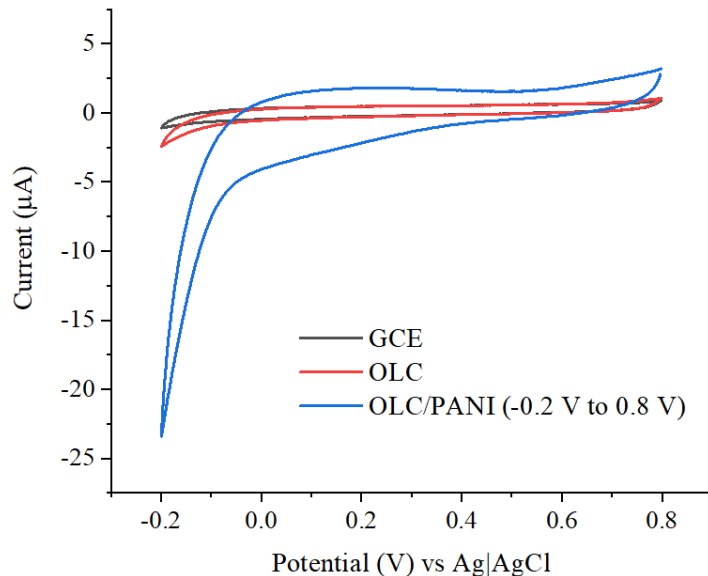


Figure 7 – Cyclic Voltammetry of OLC/PANI.

Conclusion

Through electrochemical synthesis, it was possible to polymerize the aniline monomer together with OLC nanoparticles. This was done using an environmentally friendly method with the RoDSE technique in which no oxidizing agents were used to carry out the polymerization. A change in the structure of OLC was observed when the polymerization was done up to 0.8 V vs Ag|AgCl, which was identified using TEM images after carrying out the polymerization process. In addition, Raman spectroscopy and FTIR were used to characterize the samples that consisted of carbon structures. Raman spectroscopy showed their characteristic D, G, and 2D bands. The characteristic signals of the bonds between carbon and nitrogen were also obtained in FTIR. Cyclic voltammetry showed a clear change in the OLC/PANI sample polymerized up to 0.8 V, indicating that the synthesis was successful, even though it has to be optimized in future works.

Acknowledgments

This project was supported by the National Science Foundation under award numbers 1827622 and 1849243, and an Institutional Development Award (IDeA) from the National Institute of General Medical Sciences of the National Institutes of Health under grant number P20 GM103475-14. This content is only the responsibility of the authors and does not necessarily represent the official views of the National Science Foundation, the National Institutes of Health, or the National Aeronautics and Space Administration. Undergraduate student F. N. S. F. acknowledge the National Aeronautics and Space Administration Training Grant No. NNX15AI11H (Puerto Rico Space Grant Consortium). The authors acknowledge the Puerto Energy Center at Universidad Ana G. Mendez – Gurabo Campus and Ian Gutierrez for the use of the scanning electron microscopy facilities and the Molecular Science Research Center (MSRC) at the University of Puerto Rico for the use of the Raman spectroscopy facilities.

References

1. L. Echegoyen, A. Ortiz, M. N. Chaur and A. J. Palkar, *Chem. Nanocarbons*, (2010).
2. D. Santiago, G. G. Rodríguez-Calero, A. Palkar, D. Barraza-Jimenez, G. H. Galvan, G. Casillas, A. Mayoral, M. Jose-Yacamán, L. Echegoyen and C. R. Cabrera, *Langmuir*, **28** (2012).
3. M. E. Plonska-Brzezinska, J. Mazurczyk, B. Palys, J. Breczko, A. Lapinski, A. T. Dubis and L. Echegoyen, *Chem. Eur. J.*, **18** (2012).
4. O. Mykhailiv, M. Imierska, M. Petelczyc, L. Echegoyen and M. E. Plonska-Brzezinska, M. E., *Chem. - A Eur. J.* **21**(15) (2015).
5. J. Stejskal, M. Omastová, S. Fedorova, J. Prokeš, and M. Trchová, *Polymer (Guildf)*, **44**(5), (2003).
6. E. M. Elnaggar, K. I. Kabel, A. A. Farag and A. G. Al-Gamal, *J. Nanostructure Chem*, **7**(1), (2017).
7. I. Kovalenko, D. G. Bucknall and G. Yushin, *Adv. Funct. Mater*, **20**(22), (2010).
8. N. Wang, B. Lu, L. Li, W. Niu, Z. Tang, X. Kang, and S. Chen, *ACS Catal*, **8**(8), (2018).
9. Y. Zhang, X. Zhuang, Y. Su, F. Zhang, and X. Feng, *J. Mater. Chem. A*, **2**(21), (2014).
10. A. Shaikh, B. K. Singh, D. Mohapatra, and S. Parida, *Electrocatalysis*, **10**(3), (2019).
11. L. Lai, J. R. Potts, D. Zhan, L. Wang, C. K. Poh, C. Tang, H. Gong, Z. Shen, J. Lin and R. S. Ruoff, *Energy Environ. Sci.*, **5**(7), (2012).
12. N. Zhou, N. Wang, Z. Wu and L. Li, *Catalysts*, **8**(11), (2018).
13. Z. Wu, M. Song, J. Wang and X. Liu, *Catalysts*, **8**(5), (2018).
14. L. Dai, Y. Xue, L. Qu, H. J. Choi and J. B. Baek, *Chem. Rev.* **115**(11), (2015).
15. L. Cunci, C. A. Velez, I. Perez, A. Suleiman, E. Larios, M. José-Yacamán, J. J. Watkins and C. R. Cabrera, *Appl. Mater. Interfaces*, **6**, (2014).
16. D. Santiago, G. G. Rodríguez-Calero, H. Rivera, D. A. Tryk, M. A. Scibioh, and C. R. Cabrero, *J. Electrochem. Soc.* **12**, (2010).

17. Warren, M. *Electronic and Structural Effects on the Electrochemistry of Polypyrrole*. The University of British Columbia (2005).
18. A. Palkar, F. Melin, C. M. Cardona, B. Elliott, A. K. Naskar, D. D. Edie, A. Kumbhar and L. Echegoyen, *Chem. Asian J.*, **2**, (2007).
19. I. Sapurina and J. Stejskal, *Polym Int*, **57**, (2008).
20. A. C. Ferrari and J. Robertson, *Physical review*, **61**(20), (2000).